



OPTICAL PHYSICS

Nested-ring Tm-doped high-power widely tunable fiber laser

RICHARD ŠVEJKAR,* D MARTIN P. BUCKTHORPE, PETER C. SHARDLOW, AND W. ANDREW CLARKSON

Optoelectronics Research Centre, University of Southampton, University Rd., Southampton SO17 1BJ, UK *richard.svejkar@soton.ac.uk

Received 23 July 2025; revised 19 August 2025; accepted 19 August 2025; posted 20 August 2025; published 8 September 2025

A structured thulium-doped nested-ring active fiber was used to build a widely tunable high-power fiber laser. The nested-ring fiber allows high-power cladding pumping along with enhanced thermal management, improvement in the efficiency of the two-for-one process, and enabling single-mode operation. The straightforward tunable cavity design permits remote tuning while ensuring full enclosure of free-space optics and purification with nitrogen to mitigate the effects of water vapor absorption on the lasing process. Our study introduces a tunable Tm-fiber laser capable of emitting in the 1930 to 2090 nm range with a linewidth of 0.2 nm, delivering stable output power up to 70 W.

Published by Optica Publishing Group under the terms of the Creative Commons Attribution 4.0 License. Further distribution of this work must maintain attribution to the author(s) and the published article's title, journal citation, and DOI. https://doi.org/10.1364/JOSAB.573697

1. INTRODUCTION

The wavelength range of 2 μm is crucial for biomedical applications and material processing. The broad emission band of the thulium-doped silica fiber laser enables these lasers to operate efficiently in a wavelength spectral range from 1.65 to 2.1 μm , which allows molecular water absorption lines to be selectively targeted or avoided [1–3]. Tm-doped fiber lasers have emerged as key players in various fields, e.g., medical treatment, material processing, spectroscopy, remote sensing, nonlinear conversion, LIDAR, and communication and defense systems [3,4].

The Tm³⁺ ion energy levels, see Fig. 1, exhibit a complex structure, allowing several pumping schemes to be utilized, where energy transfer and excited-state absorption processes occur. Core pumping at 1.55 µm allows access to shorter emission wavelengths [5,6]; however, from the point of view of power-scaling, cladding pumping (790 nm) is more convenient due to the power-scaling limitations of 1.55 µm pump sources, as one can see in [7]. Tm-doped systems are well known for a two-for-one cross-relaxation process, which enables the potential emission of two 2 µm signal photons for the absorption of a single 793 nm pump photon (${}^{3}H_{4} \rightarrow {}^{3}F_{4}$); Tm(${}^{3}H_{6} \rightarrow {}^{3}F_{4}$). This leads to a theoretical maximum quantum efficiency of 2 and a doubling of the theoretical maximum operating efficiency [8]. This "two-for-one" cross-relaxation process is concentration-dependent and requires a Tm3+ doping concentration in excess of 3.5 wt. % to be exploited efficiently [9]. However, the high concentration of thulium leads to a higher thermal load, hence higher demands on thermal management.

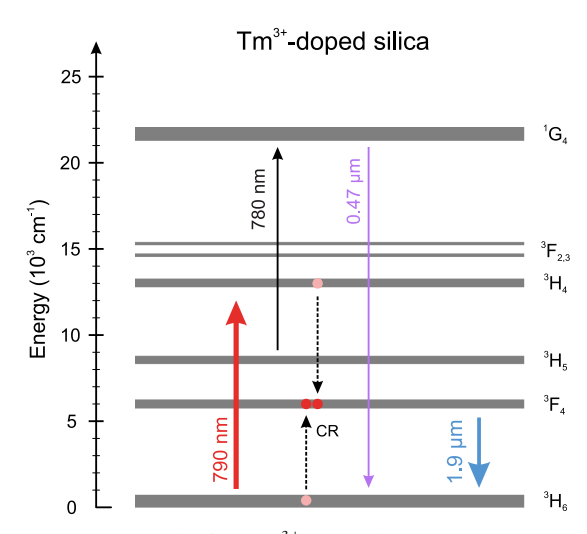


Fig. 1. Energy levels of the Tm³⁺ ion in silica. CR, cross-relaxation.

The nested-ring fiber was designed to utilize a non-uniform Tm-doping profile across the core, reducing the thermal load per unit length while also promoting efficient cross-relaxation [4].

As mentioned above, there are various applications for Tm-based lasers, from which demands arise on operation at a variety of wavelengths. This could be simply achieved by a correct combination of active fiber length and fiber Bragg grating (FBG) in the case of targeted emission at a particular wavelength. However, to enable greater flexibility, it is more convenient to design a tunable laser where the emission wavelength can be

changed continuously during laser operation within a wide spectral range. Rare-earth-doped fibers, and glass in general, are ideal matrices since they exhibit broad transitions with a bandwidth of tens of nanometers. This is given by inhomogeneous broadening, which arises from the non-uniform distribution of active ions in the host, which is typical for glasses [10]. It was shown in [5] that Tm-doped fiber lasers can be tuned across a wide range of 371 nm from 1654 to 2025 nm with maximum output reaching 8 W. However, such a broadband tuning requires a combination of core (1.55 µm) and cladding $(0.79 \mu m)$ pumping, which leads to a more complex system with relatively low output power. In [11], the authors demonstrated a high-power, tunable thulium-based fiber laser delivering about 60 W of output power but with a relatively narrow 70 nm tuning range and free-space pump coupling from both ends of the active fiber, potentially leading to additional stability concerns. An alternative approach would be the implementation of a master oscillator power amplifier (MOPA) system as presented in [12], which allows an increase in output power to 175–200 W (1927–2098 nm). However, this adds significant complexity to the design of the laser system.

Our objectives were to build a simple, compact, tunable, transportable, and enclosed laser system with an N_2 purified chamber for the tuning cavity. In this work, we present a thulium-doped fiber laser based on a nested-ring active fiber design, offering tunable output from 1.93 to 2.09 μm with up to 70 W of power when using a free-space tuning cavity, or fixed-wavelength emission at 1940 nm with up to 96 W of power when configured with a high-reflectivity fiber Bragg grating (HR FBG).

2. MEASUREMENTS AND METHODS

As mentioned above, the tunable Tm-fiber laser is based on a structured nested-ring fiber that was designed, prepared, and drawn at the University of Southampton laboratories. The fiber is designed to match passive double-clad fibers with the 10/125 µm core/cladding diameter and with a numerical aperture of 0.15/0.46. The fiber specifications are as follows: concentration of Tm^{3+} 4 wt.%, core size 8.2 μ m (NA = 0.15), an octagon-shaped cladding with dimensions 122 (flat-toflat diameter) and 132 µm (corner-to-corner diameter) with cladding NA 0.46. Complete fiber specifications and more details about this type of structured fiber can be found in [4]. Confining Tm³⁺ doping to a thin ring near the outer core reduces overlap with the fundamental mode, lowering gain for parasitic emission at longer wavelengths and enabling efficient short-wavelength operation. Although the effect on parasitic suppression is modest in our nested-ring fiber, the design significantly reduces thermal loading by lowering pump absorption per unit length while maintaining high Tm³⁺ concentration (4 wt. %) for efficient "two-for-one" cross-relaxation. This approach allows higher output power before thermal limits, typically set by polymer coating degradation, are reached. The active fiber was wound to an aluminum mandrel, which was fastened to a cold plate and maintained at 18°C.

Two fiber-coupled nLight diodes (element e18, 90 W at 793 nm, and $105/125~\mu m$) were combined in a Gooch & Housego tapered fiber bundle (TFB-Z00612A82, 6+1:1,

signal fiber 10/125 μm, NA 0.15 and pump fibers 105/125 μm, NA 0.22). Hence, there is the option for further power scaling with the integration of additional pump diodes. The total incident pump power corrected for Fresnel losses behind the combiner was 191 W. The output feed through the fiber of the combiner was spliced onto 6.35 m of active Tm-fiber. The combiner input fiber that led to the free-space tuning cavity of the system was spliced to a cladding mode stripper (CMS) to remove residual pump light. The opposite pigtail of the CMS was protected and terminated by an anti-reflection (AR) coated end-cap. The passive fiber was bonded to the end-cap in our laboratory by a home-made fiber end-capping system. The free-space part of the laser cavity consists of an aspheric lens (ZnSe, f = 25 mm), Ibsen transmission grating (PCG-560-2000-934, grating resolution 560 l/mm, diffraction efficiency >90% at 1.90-2.15 µm, designed AOI 34°), an achromatic doublet lens (f = 75 mm), a prism slit, and an HR mirror (HR at 1.8–2.1 μm). An achromatic doublet lens was used to suppress chromatic aberration, preserving tuning stability across the full range by minimizing effects on the free-space section of the laser. An aspheric lens was selected to maintain a diffraction-limited beam and enable optimal coupling into the single-mode fiber. The free-space cavity was placed in an enclosed chamber that was purified with nitrogen to minimize the absorption effects of water vapor in the air. The opposite end of the active fiber was spliced to a matching passive fiber, where the output coupler was formed by a flat cleave with reflectivity given by Fresnel losses of 3.4%. At the fiber laser output, residual pump light was separated from the signal using a dichroic mirror. The complete experimental layout can be seen in Fig. 2 together with the inset image of the nested-ring fiber. The emitted laser wavelength during tuning experiments was measured using a Yokogawa optical spectral analyzer (AQ6375, 1.2-2.4 μm, 50 pm resolution).

There are various methods for constructing a tuning cavity; however, each of which relies on either amplitude or angle selection of wavelength [10,13]. The former approach leverages the dependency of transmission or reflection on elements inserted in the resonator, such as dielectric filters or birefringent plates. A typical example would be an intracavity-placed birefringent plate under Brewster's angle inserted within active media and output coupler (OC) [14]. By rotating the birefringent plate with respect to its normal plane, one can tune the emitted wavelength. The latter relies on the spatial dispersion of light, achievable through prisms or gratings. A typical representative system features reflective diffraction gratings arranged in the Littrow configuration to provide feedback [5,6]. Here, the wavelength is changed by slightly angling the grating, which also acts as a back-reflecting mirror.

Both the above-mentioned approaches require moving one of the components directly involved in the resonator as an active optical element, i.e., rotating a birefringent plate, an angle grating, or a prism. This could affect the stability of the emitted wavelength and output power arising from temperature fluctuation and vibration, which could lead to potential misalignment of the system.

Our cavity has been engineered so that there is no need to move either of the optical components through the implementation of a transmission grating. The only moving part within

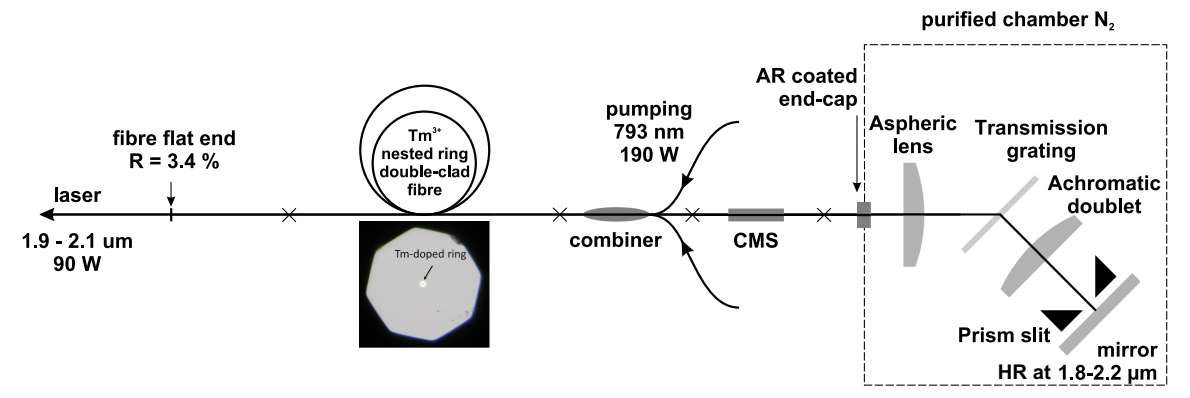


Fig. 2. Scheme of the experimental setup.

the resonator is a sideways translation of a slit created by two glass prisms, which solely serves to select the wavelength and is not directly engaged as an active element. The pair of glass prisms was selected to avoid potential damage that could result from the high intra-cavity power if a metal slit were used. Using transmission gratings ensure a more robust system solution because they are less sensitive to angle misalignment [13]. This approach enhances overall laser stability and minimizes wavelength drift, as individual diffraction orders remain fixed when the transmission grating is rotated. The transmission diffraction grating used in the setup was designed to be used for the 2 μm wavelength region as well as so that diffraction occurs primarily in the first order. This has allowed a robust and stable laser system design.

3. RESULTS AND DISCUSSION

First, the laser was built in an all-fiber configuration emitting at a fixed wavelength of 1940 nm using an FBG, which was spliced to the combiner instead of the CMS. This setup was used to test up to a maximum pump load and test all splices. Results presented in Fig. 3 show a maximum output power of 96 W with a slope efficiency of 55% with respect to absorbed power. The following step was to build the free-space part with the HR mirror, which was placed behind the aspheric lens. This was done to test free-space coupling up to the maximum pump and output laser power. One can see in Fig. 3 that the slope efficiency of 45% and maximum output power of 76 W are comparable with the results for the complete tunable free-space cavity. The emission wavelength, without any slit, for the HR mirror and full tuning cavity setup was 2010 nm. In both setups, laser emitted radiation was in the fundamental mode with $M^2 = 1.07$, which is to be expected as the output was a single-mode fiber.

The main limiting factors from the point of view of efficiency were the transmission grating, which has diffraction efficiency >90%, and the AR-coated bulk end-cap. The latter mentioned a slightly distorted beam due to imperfect bonding between the passive fiber and the bulk optic. This results in less effective back coupling, heating, and decreasing efficiency and power loss.

In the next step, with a full tuning cavity, wavelength tuning was tested, the results of which are shown in Fig. 4. The free-space part of the laser oscillator was enclosed and purified with nitrogen to avoid the influence of water vapor absorption on the

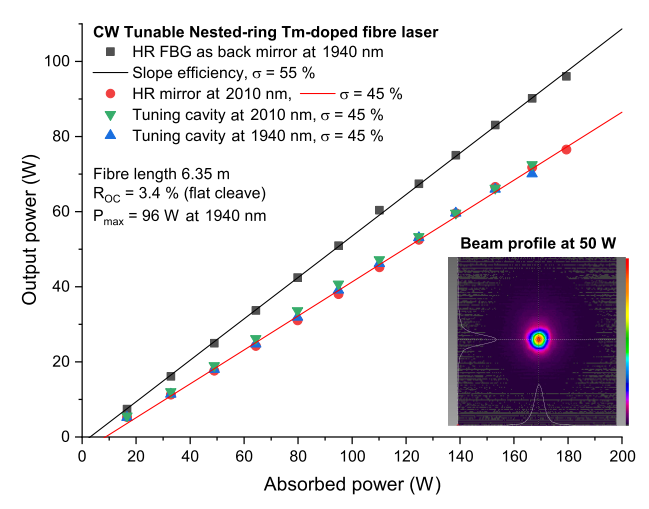


Fig. 3. Output laser characteristics for CW laser operation; σ , slope efficiency; λ_{pump} , pumping wavelength; P_{max} , maximal output power; $\Delta \lambda$, tuning range; R_{OC} , output coupler reflectivity.

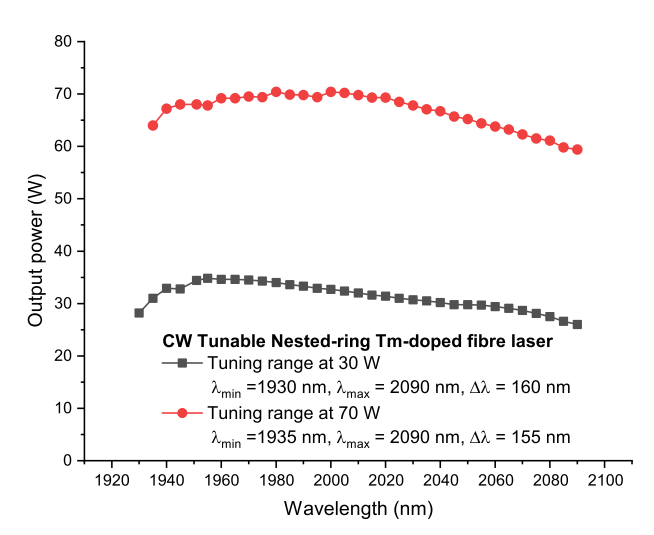


Fig. 4. Power tuning curve of the laser for two output power levels; $\Delta \lambda$, tuning range.

tuning range and output power. The slit was set parallel to the HR mirror, and the tuning was realized by translating the slit sideways. Based on the grating and free-space optics parameters,

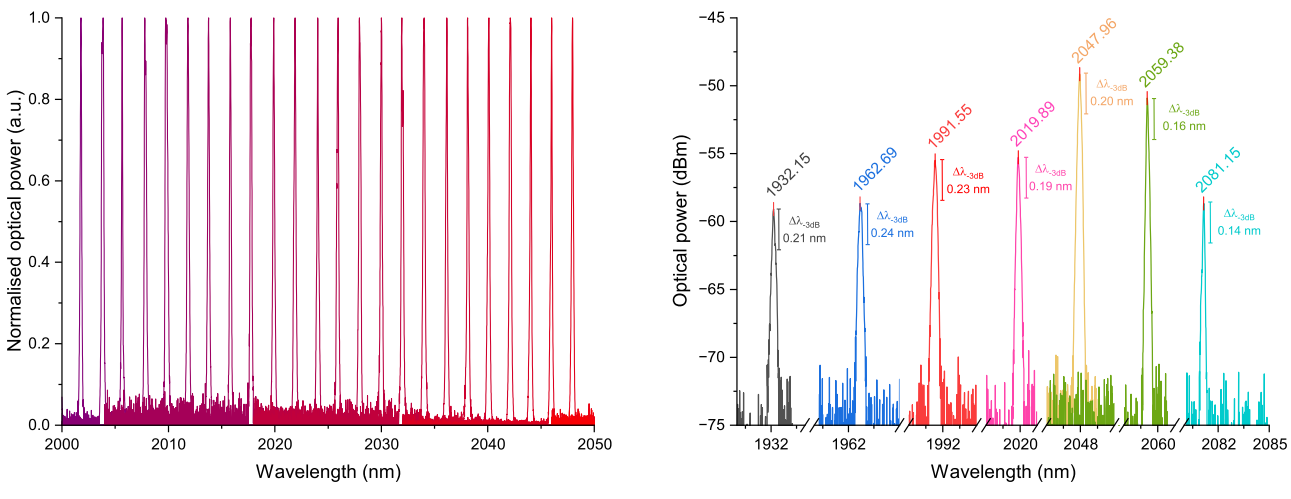


Fig. 5. Tuning curve of the laser for the spectral range of 2000–2050 nm and detailed graph of several emission lines; $\Delta \lambda_{-3 \text{ dB}}$, linewidth at -3 dB.

the minimal linewidth was initially estimated to be $0.4\,\mathrm{nm}$. However, a slightly narrower linewidth of $0.2\,\mathrm{nm}$ was achieved, and it was possible to maintain it across the entire tuning range. The emission lines, presented in Fig. 4, show a wavelength range of $2000-2050\,\mathrm{nm}$. The presented narrower spectral range was chosen to make the graph readable; the whole dataset is available online in the technical data file. Details of several emission lines together with marked $-3\,\mathrm{dB}$ linewidth can be seen in Fig. 5. The laser setup allows varying the emission linewidth in the range of $0.2-1.5\,\mathrm{nm}$ while maintaining single-wavelength operation. The change in linewidth was realized by changing the separation of the glass prism that forms the slit.

The overall tuning range is limited by the range of slit translation, as at the extremities, the slit starts to block the laser beam. Output power and efficiency decrease beyond 2030 nm is likely due to reaching the tail of the thulium emission band and to increased core propagation loss at longer wavelengths. The maximum tuning range at 30 W of output power was 160 nm from 1930 to 2090 nm. It was possible to reach a stable tuning curve up to 60-70 W spanning from 1935 to 2090 nm. The laser was operated for more than 30 min without any power or wavelength variation or degradation. The long-wavelength limit is determined by the onset of parasitic lasing at shorter wavelengths. Operation at shorter wavelengths is theoretically possible but would require a different set of free-space optical components and a shorter active fiber. Furthermore, the diffraction efficiency of the transmission grating falls below 90% at wavelengths shorter than 1900 nm and continues to decrease.

4. CONCLUSION

We have presented a high-power widely tunable fiber laser based on the structured Tm-doped nested-ring active fiber. The tunable laser generated CW radiation in the fundamental mode with output power reaching 60–70 W in a spectral range from 1935–2090 nm with a stable linewidth of 0.2 nm. The laser has been operated for tens of minutes without variation of output power or wavelength. The design of the tuning cavity represents a robust and straightforward solution for stable high-power tunable lasers that can be fully enclosed, purified with nitrogen,

and operated remotely. We believe that this resonator design will allow further power scaling across the tuning range. In future experiments, this tunable source will be used as the pump laser for spectroscopy measurements of Tm- and Ho-doped fibers as well as a seed source for MOPA systems.

Funding. Engineering and Physical Sciences Research Counci (EP/W028786/1).

Acknowledgment. This research was supported by the Engineering and Physical Sciences Research Council project reference EP/W028786/1, Smart Fibre Optics High-Power Photonics (HiPPo).

Disclosures. The authors declare no conflicts of interest.

Data availability. Data underlying the results presented in this paper are available at [15].

REFERENCES

- C. Romano, D. Panitzek, D. Lorenz, et al., "High-power thulium-doped fiber MOPA emitting at 2036 nm," J. Lightwave Technol. 42, 394–398 (2024).
- M. Michalska, P. Honzatko, P. Grzes, et al., "Thulium-doped 1940and 2034-nm fiber amplifiers: towards highly efficient, high-power all-fiber laser systems," J. Lightwave Technol. 42, 339–346 (2024).
- A. Sincore, J. D. Bradford, J. Cook, et al., "High average power thulium-doped silica fiber lasers: review of systems and concepts," IEEE J. Sel. Top. Quantum Electron. 24, 0901808 (2018).
- M. J. Barber, P. C. Shardlow, P. Barua, et al., "Nested-ring doping for highly efficient 1907 nm short-wavelength cladding-pumped thulium fiber lasers," Opt. Lett. 45, 5542–5545 (2020).
- M. D. Burns, P. C. Shardlow, and W. A. Clarkson, "Widely-tunable operation of a thulium doped fibre laser between 1654 nm and 2025 nm," in Conference on Lasers and Electro-Optics Europe and European Quantum Electronics Conference (CLEO/Europe-EQEC) (2021), pp. 1.
- J. Pokorný, J. Aubrecht, B. Jiříčková, et al., "Thulium-doped fiber amplifier optimized for wavelengths beyond 1800 nm," Proc. SPIE 12573, 70–75 (2023).
- D. Y. Shen, J. K. Sahu, and W. A. Clarkson, "High-power widely tunable Tm:fibre lasers pumped by an Er,Yb co-doped fibre laser at 1.6 μm," Opt. Express 14, 6084–6090 (2006).
- T. Walbaum, M. Heinzig, T. Schreiber, et al., "Monolithic thulium fiber laser with 567 W output power at 1970 nm," Opt. Lett. 41, 2632–2635 (2016).

- P. F. Moulton, G. A. Rines, E. V. Slobodtchikov, et al., "Tm-doped fiber lasers: fundamentals and power scaling," IEEE J. Sel. Top. Quantum Electron. 15, 85–92 (2009).
- R. Paschotta, Encyclopedia of Laser Physics and Technology (Wiley-VCH, 2008).
- 11. C. Guo, D. Shen, J. Long, et al., "High-power and widely tunable Tm-doped fiber laser at 2 μ m," Chin. Opt. Lett. 10, 091406 (2012).
- 12. T. S. McComb, R. A. Sims, C. C. C. Willis, et al., "High-power widely tunable thulium fiber lasers," Appl. Opt. 49, 6236–6242 (2010).
- 13. F. J. Duarte, ed., *Tunable Lasers Handbook*, 1st ed. (Academic Press, 1995).
- R. Švejkar, J. Šulc, H. Jelínková, et al., "Diode-pumped laser tunable at 2.7 μm," Opt. Mater. Express 8, 1025–1030 (2018).
- R. Švejkar, "Data in support of the 'Nested-ring Tm-doped highpower widely tunable fibre laser'," University of Southampton (2025), https://doi.org/10.5258/SOTON/D3615.